Probabilistic Flux Analysis of Cerebral Longitudinal Atrophy

Marco Lorenzi, Giovanni B. Frisoni, Nicholas Ayache, Xavier Pennec

Probabilistic flux analysis of cerebral longitudinal atrophy.

Marco Lorenzi[1,2], Giovanni B. Frisoni[2], Nicholas Ayache[1], and Xavier Pennec[1]
for the Alzheimer's Disease Neuroimaging Initiative *

[1] Project Team Asclepios, INRIA Sophia Antipolis, France
[2] LENITEM, IRCCS San Giovanni di Dio, Fatebenefratelli, Italy

Abstract. The accurate monitoring of the structural changes in the brain plays a central role in the treatment of Alzheimer's disease (AD), for instance for diagnostic purposes and for the assessment of the drugs efficacy in clinical trials. We propose here a framework based on the flux analysis of vector fields [13] for the automatic quantification of the longitudinal regional atrophy in the brain. In particular, we present here the LCC-Demons algorithm for the symmetric and robust diffeomorphic registration, which is used to quantify the longitudinal changes of a given subject by registration of follow-up images. The flux of the associated deformation across the boundaries of consistently defined group-wise regions provides the rate of longitudinal volume change. The proposed method was tested for the quantification of the longitudinal hippocampal and ventricular volume changes at one and two years from baseline from a group of AD and healthy ADNI subjects. The resulting measures led to statistically powered results, and to consistent longitudinal measures in terms of symmetry, transitivity and linearity.

1 Introduction

Alzheimer's disease (AD) is a neurodegenerative pathology of the brain, characterized by a co-occurrence of different phenomena, starting from the deposition of amyloid plaques and neurofibrillary tangles, to the development of functional loss, to finally cause the cell death [9]. Among these pathological changes, the cerebral atrophy measured through magnetic resonance (MR) is usually identified as the "footprint" of the disease which may become dramatic in the latest stages, but which it has been shown to start before the clinical conversion to AD, already at early and premorbid stages [17]. As a consequence, the monitoring of the brain structure has been included in the list of recommended diagnostic criteria [3], and the volume changes of key areas like the hippocampus are now

* Data used in preparation of this article were obtained from the Alzheimer's Disease Neuroimaging Initiative (ADNI) database (www.loni.ucla.edu/ADNI). As such, the investigators within the ADNI contributed to the design and implementation of ADNI and/or provided data but did not participate in analysis or writing of this report. A complete listing of ADNI investigators can be found at:www.loni.ucla.edu/ADNI/Collaboration/ADNI_Authorship_list.pdf

employed as surrogated biomarker in clinical trials. The MR imaging is thus a fundamental instrument for the clinical practice, which is also cheaper and more feasible then other imaging modalities. Therefore, the development of robust tools for the analysis of MRIs is now a central field of research in the medical imaging. For this purpose, an important contribution came from the recent availability of public longitudinal studies like the "Alzheimer Disease Neuroimaging Initiative" (ADNI)[14], which provides the research of data representing the complete history of the Alzheimer's pathological process: from the healthy condition to mild cognitive impairment (MCI), to finally reach the advanced stages of the disease.

Among the different techniques for the quantification of the brain structural changes we can identify segmentation based approaches (like the Boundary Shift Integral (BSI) [6] or SIENA [19]), and non-rigid registration based ones (for instance voxel compression maps (VCM) [4], RAVENS maps [16] and cortical pattern matching (CPM) [20]). Non-rigid registration is a powerful instrument which found application in several research context, since it provides a rich description of the atrophy process which ranges from the local (voxel) to the regional level. However, in spite of its large employment in research, non-rigid registration is not very diffuse in the clinical setting, for example for the longitudinal atrophy quantification in clinical trials. This is partly due to the higher technical requirements asked in the clinical context in terms of accuracy, robustness to the biases affecting the medical images, and stability of the measures over time. The failing in controlling these factors inevitably leads to the decreased sensibility of the atrophy measures, and thus to the potential failing or increase in cost of the trial.

The scenario was recently pointed in [5]. This interesting paper identifies a set of "quality criteria" that an imaging tool should satisfy in order to find application in the clinical setting:

- *Biological plausibility.* The algorithm should provide atrophy measurements consistent with the known pathophysiology.
- *Symmetry.* The atrophy quantified from A to B should be consistent with the one quantified from B to A.
- *Transitivity.* The atrophy quantified from A to C should be equivalent to the cumulative one from A to B and B to C.
- *Comparison with the "state of art".* The atrophy measurements should be validated on shared data and compared to those obtained from more established algorithms.
- *Reproducibility on back-to-back images.* The group average on same days scans should be zero.
- *Statistical validation.* The accuracy of the measurements should be evaluated by sample size analysis based on the differential progression between AD and normal aging.

In [13] we proposed the regional flux analysis of the one-year changes in AD, based on non-rigid registration of follow-up images. The framework automatically defines a set of consistent group-wise atrophy regions for AD, which

are then used to provide powered measurements of the longitudinal structural changes. In light of these encouraging results, it is therefore interesting to assess the reliability of the flux analysis on the above mentioned "quality criteria", and to benchmark it on public data with respect to validated methods. However, since the flux analysis proposed in [13] does not rely on prior hypothesis on the location of the regional atrophy, a different approach should be introduced for the atrophy quantification in apriori regions.

Aim of this work is to provide a framework based on the flux analysis for the quantification of the longitudinal atrophy in the hippocampi and ventricles. In Section 2 we introduce the LCC-Demons, a registration algorithm for the robust and symmetric diffeomorphic image registration, and in Section 3 we recall the basic concepts of the flux analysis of deformation fields. Based on these contributions, we detail in Section 4 the proposed framework for the quantification of the regional longitudinal atrophy. Finally, in Section 5 we validate the framework by testing the above criteria on the ADNI longitudinal images (baseline, 12, and 24 months) from a group of healthy subjects and AD patients.

2 LCCDemons: Symmetric Local Correlation Criteria in the log-Demons.

The robustness to the bias affecting the medical images is a fundamental requirement for the reliable estimation of the observable anatomical changes. For example, to accurately detect the morphological differences through non-rigid registration we need to not mistake spurious intensity differences as anatomical ones. This is usually achieved by opportunely defining similarity criteria which can cope with noise. In this work we address this problem by proposing the symmetric LCC-Demons, a modified version of the symmetric diffeomorphic Demons (or log-Demons) algorithm [21], which implements the local correlation coefficient in order to locally model additive plus multiplicative intensity bias.

The log-Demons. The standard log-Demons algorithm performs diffeomorphic registration parametrized by stationary velocity fields. The registration of a pair of images is achieved through an alternate optimization scheme. First, the *correspondence step* optimizes the sum of squared differences of the intensities (SSD) between the images by estimating an unconstrained correspondence encoded by the exponential $\exp(\mathbf{v_x})$ of the stationary velocity field $\mathbf{v_x}$. Second, the *regularization step* estimates the transformation parameters that best explains the correspondence field using a penalized least-squares approach. The regularity criterion is an infinite order differential quadratic form of the velocity field [1], whose optimum is obtained through a Gaussian convolution of smoothing parameter $\sigma_{elastic}$. An additional (so-called fluid) regularization step with parameter σ_{fluid} is often performed when updating the correspondences in addition to the elastic-like penalization.

The LCC-Demons. The correspondence $\exp(\mathbf{v_x})$ of the log-Demons is based on the minimization of the SSD, which is known to be sensitive to the local biases and thus not reliable for anatomical quantification. By following [2] we replaced the SSD in the log-Demons by the local correlation coefficient (LCC):

$$\rho(I,J) = \frac{\overline{IJ}}{\sqrt{\overline{I^2}\,\overline{J^2}}},$$

where $\overline{I} = \int_\Omega \mathbf{G}_{\sigma_L} * I(\omega)\, d\omega$ is the local image mean defined by convolution with a Gaussian kernel of size σ_L.

The LCC criteria is robust to affine intensity changes (i.e. to additive and multiplicative bias) and is local, thanks to the Gaussian weights $\mathbf{G}_{\sigma_L}$. This is a rather interesting feature, since the noise is modeled here as a spatially varying process whose degree of variation is controlled by the kernel size σ_L (smaller σ_L to account for more local noise). In this way, no bias field removal is needed as preprocessing step prior to the non-rigid registration.

In order to not introduce bias due to the asymmetric processing of the images, it is preferable to be independent from the order considered for fixed and moving image [22]. We can address this point by taking advantage of the log parametrization of the correspondence field $\exp(\mathbf{v_x})$. In fact, a symmetric optimization scheme can be obtained by resampling both images in the "half-way" space: $I \circ \exp(-\frac{\mathbf{v_x}}{2})$ and $J \circ \exp(\frac{\mathbf{v_x}}{2})$. This scheme is therefore independent by the choice of the pair order, and provides a perfectly symmetric displacement field.

It can be shown that by integrating the proposed symmetric LCC criteria into the log-Demons registration we obtain a close form solution for the Gauss-Newton optimization of the correspondence step, and thus we preserve the log-Demons numerical efficiency. We measured an average computational time for the registration of a couple of brain images (image resolution 182x218x182, voxel size 1x1x1) of around 20 minutes on an AMD Opteron dual core 2000Mhz.

The registration parameters used in the following experiments are: $\sigma_L = 2$ voxels, $\sigma_{elastic} = 1$ voxel, and $\sigma_{fluid} = 0.5$, voxels with a multiresolution optimization scheme of 30x20x10 iterations from coarser to finer resolution.

3 Vector Field Divergence to Quantify the Observed Atrophy

Let consider the longitudinal changes between a pair of follow-up brain images estimated by the LCCDemons non-rigid registration. The associated diffeomorphism $\varphi = \exp(\mathbf{v})$ densely represents the local atrophy as a complementary compression/expansion process across adjacent areas. The compression models the shrinking of the anatomical structures due to the observed matter loss, while the expansion is a complementary process which indicates growth, for instance of the CSF areas in the ventricles, or in the sulci surrounding the gray matter.

These processes are induced by the estimated deformation field and can be quantified by the flux of the vectors across the boundary of the regions: the inward (resp. outward) flow across a surface induces the compression (resp. expansion), which quantifies the atrophy (resp. growth).

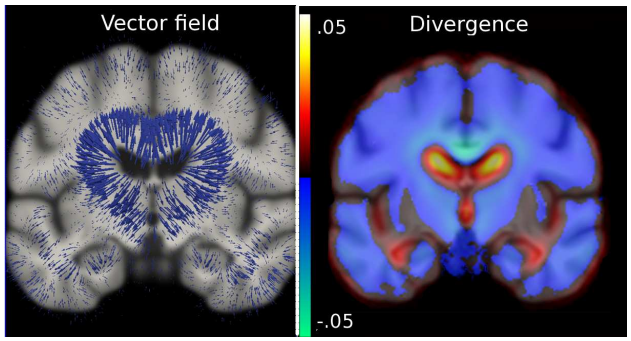

Fig. 1: Divergence associated to a vector field. Left: vector field of a longitudinal deformation in Alzheimer's disease. Ventricles and temporal lobes are the region of higher flux (vector flow) from the CSF areas to the gray/white matter ones. Right: Divergence associated to the vector field. The areas of maximal/minimal divergence (ventricles, temporal lobes) are those of higher volume change.

The flux is is the mathematical formulation of the boundary shift, and is identified by the divergence $\nabla \cdot \mathbf{v}$ associated to the field $\mathbf{v}$ (Figure 1). In fact, from the Divergence (or Ostrogradsky's) theorem, the integral of the divergence of a vector field in a given region is the flux of the vector field across the boundaries of the region. The rate of volume change of the region is then the integral of the divergence over the volume:

$$\frac{\int_\Omega \nabla . \mathbf{v} \, d\omega}{\int_\Omega d\omega} = \frac{\int_{\partial\Omega} \mathbf{v} \cdot \mathbf{n} \, ds}{Vol(\Omega)},$$

We finally note that the areas of maximal/minimal divergence automatically identify the spatial locations of expansion/compression, i.e. involved in the process of matter loss[13]. In the following, the divergence associated to the pair-wise deformations is used to localize the areas of relevant longitudinal atrophy and to quantify the associated rate of volume change.

4 Measurement of the Hippocampal and Ventricular Longitudinal Changes in AD

Given a sequence of follow-up images I_i $(i = 0, \ldots, N)$ for a given subject, the proposed framework is composed by the following steps.

Alignment of the Sequence to the Template Space. In this step (Processing Step 1) the images are aligned and normalized to a pre-defined anatomical template estimated from a group of healthy elderly subjects of the ADNI cohort. The alignment to the Template space is needed for the subsequent propagation of the anatomical regions through non-rigid registration. The global affine transformation is estimated by the FLIRT software [10]. The resampling is performed by linear interpolation on the intensities.

Processing Step 1 Consistent alignment of the time series.

Given a sequence of follow-up images I_i $(i = 0, \ldots, N)$:

1. Estimate the "9 parameters affine" global transformation to the baseline $A_i : I_0 \simeq I_i \circ A_i$ $(i = 0, \ldots, N)$.
2. Skull strip the baseline I_0 (ROBEX software [8]).
   Mask the I_i $(i = 0, \ldots, N)$ with the estimated brain mask to get I_i^M.
3. Refine the initial transformation.
   Estimate the "9 parameters affine" global transformation A_i^M: $I_0^M \simeq I_i^M \circ A_i^M$ $(i = 0, \ldots, N)$.
4. Register the baseline I_0^M to the template space T.
   Estimate the 12 parameters global affine transformation A_0^T: $T \simeq I_0 \circ A_0^T$.
5. Compute the aligned time series $I_i^T = I_i \circ \left(A_0^T \circ A_i^M \circ A_i\right)$.

We notice that all the images undergo only one interpolation, and are therefore consistently processed in order to not introduce biases on the intensities due to asymmetric resamplings [22].

Definition of Consistent Spatial Regions of Atrophy. Prior group-wise regions for the quantification of the hippocampal and ventricular longitudinal changes were defined in the template space T. The regions were estimated from a mixture of anatomical segmentation and of prior information of the longitudinal AD atrophy. The longitudinal atrophy in AD was estimated from a group of AD patients from the ADNI dataset [12], and is here quantified by the divergence of the modeled average longitudinal progression (Figure 2A'). The regions were defined as follow:

- Region of ventricular expansion R_v. The prior region of ventricular expansion was decomposed in two complementary parts $R_v = R_{v-} \cup R_{v+}$ (Figure 2A) of respectively compression and expansion (red and yellow in the figure). These areas are defined by the maximal and minimal average divergence (Figure 2A') within a predefined ventricle mask (Figure 2A", blue).
- Region of hippocampal atrophy R_h. The prior region of longitudinal hippocampal atrophy was decomposed in two complementary parts $R_h = R_{h-} \cup R_{h+}$ of respectively hippocampal atrophy and temporal horn expansion. The first one (R_{h-}) is the anatomical mask of the hippocampi computed by segmentation propagation in the template space of the automatically segmented

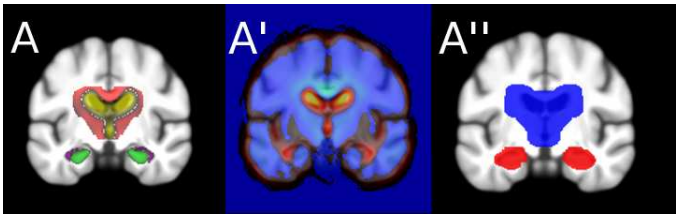

Fig. 2: Prior region of longitudinal atrophy in AD. A) Prior anatomical areas for the hippocampal (purple and green), and ventricular (yellow and red) expansion and contraction. A') Average divergence map for the longitudinal atrophy in AD (from [12]). A") Ventricular and hippocampal mask for the extraction of the maximal/minimal divergence areas.

ADNI subject-specific hippocampal masks [15] (Figure 2A, green). The resulting probabilistic hippocampal mask is the area for the quantification of the longitudinal matter loss. The second one (R_{h+}) is defined similarly for the ventricles from the locations of maximal average divergence in the hippocampal mask (Figure 2A" red), and encodes the expansion of the temporal horn which is complementary to the hippocampal atrophy (Figure 2A purple).

The subject specific regional longitudinal changes are computed by following the Processing Step 2.

Processing Step 2 Quantification of subject-specific regional atrophy.

Given the sequence of aligned follow-up images I_i^T $(i = 0, \ldots, N)$:

1. Non linearly register the follow-up images to the baseline with the LCC-Demons algorithm. Estimate v_i such that $I_0^T \simeq I_i^T \circ \exp(v_i)$.
2. Compute the average longitudinal divergence map $D = \overline{\nabla . v_i}$.
3. Transport the prior regions R_h and R_v in the subject space through the subject-to-template deformation to define R_v^s and R_h^s.
4. Restrict the hippocampal region to the subject specific areas of compression/expansion:
$$R_{h-}^s \cap \{x | D(x) < 0\},$$
$$R_{h+}^s \cap \{x | D(x) > 0\}.$$
5. Define the atrophy rate at the time point i as the algebraic sum of the average divergence D_i in the compression and expansion areas of the resulting ventricular and hippocampal regions.

---

5 Longitudinal Atrophy on the ADNI Dataset.

The presented method was applied for the quantification of the longitudinal hippocampal atrophy in a sample of 96 AD subjects and 160 healthy controls

from the ADNI dataset. Images of 0, 12, and 24 months were aligned according to the Step 1 and the longitudinal atrophy was evaluated as in Step 2 to test the following quality criteria:

- *Consistency with the clinical condition.* As indicated by Table 1 the AD group has significantly higher ventricular expansion and hippocampal atrophy for all the considered intervals ($p < 0.001$, standard t-test). The estimated atrophy rates are consistent with those reported in literature [7,18,11].

	Hippocampi		Ventricles	
	Ctrls	AD	Ctrls	AD
[0-12]	2.38 (1.64)	5.28 (2.38)	1.89 (2.09)	4.03 (2.79)
[0-24]	3.52 (2.04)	10.09 (4.5)	3.56 (2.82)	8.9 (5.32)
[12-24]	1.19 (1.4)	4.89 (2.94)	1.72 (2.19)	4.9 (3.3)

Table 1: Estimated percentage atrophy rates (SD) in the ventricular and hippocampal regions for the pairs T12-T0, T24-T0, and T24-T12.

- *Symmetry.* The longitudinal atrophy measure is perfectly symmetric, due to the symmetry of the registration algorithm. Therefore the absolute changes measured from A to B are equal (with opposite sign) to those from B to A.
- *Linearity over two years.* Table 2, first row, shows the estimated mean and standard deviation for the ratio of the estimated atrophy between 2- and 1-year atrophy rate. The ratios are never significantly different from the reference value of 2.
- *Transitivity.* Table 2, second row, shows the compatibility in time of the atrophy measures computed as the error between the measure from A to C and the cumulative one from A to B and B to C. As indicated, the transitivity error is never significantly different from 0, even though it is close to significance for the hippocampal atrophy in AD. We notice that this error is however small relatively to the atrophy rate at 24 months (about 1%).
- *Sample size analysis.* Based on the reported atrophy rates, we estimated the sample size required to detect a 25% difference in the AD longitudinal progression relative to the normal aging (80% power, 0.05 significance). The sample size (Table 3) are in line with those reported in the previous studies [11,18].

6 Conclusions.

We presented a framework based on the flux analysis of vector fields for the quantification of the longitudinal hippocampal and ventricular changes in AD. The framework estimates the longitudinal changes by non-rigid registration performed by the LCC-Demons, a robust and symmetric non-rigid registration algorithm, and quantifies the atrophy by integration of the flux of the vector fields on

	Hippocampi		Ventricles	
	Ctrls	AD	Ctrls	AD
[0-24]/[0-12]	1.77 (1.19)	1.98(0.67)	1.48 (5.65)	2.65 (3.96)
p	0.44	0.8	0.39	0.11
[0-12]+[12-24]-[0-24]	0.04 (0.3)	0.09 (0.5)	0.05 (0.61)	0.08 (0.75)
p	0.1	0.08	0.28	0.3

Table 2: Linearity and transitivity of the estimated atrophy rates. First row: mean (SD) of the ratio 2-years over 1-year atrophy. The p-value indicates the significance of the difference relative to the reference value of 2. Second row: mean (sd) of the transitivity error. The p-value indicates the significance of the difference relative to 0 (paired t-test).

	[0-12]	[0-24]
Hippocampi	169 (119,255)	117 (89,162)
Ventricles	426 (249,880)	249 (168,410)

Table 3: Sample size analysis provided by the estimated atrophy rates. Average sample size (95% CI) to detect a 25% difference in the AD progression relative to the normal aging with 80% power and significance level of $p = 0.05$.

consistently defined group-wise regions. Experimental results indicate accurate and consistent quantification of the longitudinal atrophy, which lead to statistically powered results. The proposed method does not rely on the segmentation of the anatomical structures, but is based on the propagation of prior regions of longitudinal atrophy defined in a template space. Thus it can be easily adapted for the atrophy quantification in different areas, identified in a general way. For instance, the ventricular region used in this work was defined from the divergence estimated in a previous study. Such a region is consistent with the registration framework and represents the expected areas of longitudinal atrophy and CSF expansion. Being able to easily define more general regions might be of relevant importance in a clinical trial setting, since it allows the investigation of the drug efficacy on more complex atrophy patterns than the one provided by the single measurement from a specific region, and might finally lead to more accurate and powered quantifications.

References

1. Cachier, P., Ayache, N.: Isotropic energies, filters and splines for vectorial regularization. J. of Math. Imaging and Vision 20, 251–265 (2004)
2. Cachier, P., Bardinet, E., Dormont, D., Pennec, X., Ayache, N.: Iconic feature based nonrigid registration: the PASHA algorithm. Computer Vision and Image Understanding 89(2-3), 272–298 (2003)
3. Dubois, B., Feldman, H., Jacova, C., et al.: Research criteria for the diagnosis of Alzheimer's disease: revising the NINCDS-ADRDA criteria. Lancet Neurol 6, 734–746 (2007)

4. Fox, N., Crum, W., Scahill, R., Stevens, J., Janssen, J., Rossnor, M.: Imaging of onset and progression of Alzheimer's disease with voxel compression mapping of serial magnetic resonance images. Lancet 358, 201–205 (2001)
5. Fox, N., Ridgway, G., Schott, J.: Algorithms, atrophy and Alzheimer's disease: Cautionary tales for clinical trials. NeuroImage 57(1), 15–18 (2012)
6. FreeBorough, P., Fox, N.: The boundary shift integral: An accurate and robust measure of cerebral volume changes from registered repeat MRI. IEEE Transaction on Medical Imaging 16(5) (1997)
7. Frisoni, G., Fox, N., Jr, C.J., Scheltens, P., Thompson, P.: The clinical use of structural MRI in Alzheimer disease. Nat Rev Neurol 6, 67–77 (2010)
8. Iglesias, J., C.Liu, Thompson, P., Tu, Z.: Robust brain extraction across datasets and comparison with publicly available methods. IEEE Trans. Med. Imaging 30(9), 1617–1634 (2011)
9. Jack, C., Knopman, D., Jagust, W., et al.: Hypothetical model of dynamic biomarkers of the Alzheimer's pathological cascade . Lancet Neurol 9(1), 119–128 (2010)
10. Jenkinson, M., Smith, S.: A global optimisation method for robust affine registration of brain images. Medical Image Analysis 5(2), 143–156 (2001)
11. Leung, K., Barnes, J., Ridgway, G., Bartlett, J., et al.: Automated cross-sectional and longitudinal hippocampal volume measurement in mild cognitive impairment and Alzheimer's disease. NeuroImage 51(4), 1345–1359 (2010)
12. Lorenzi, M., Ayache, N., Frisoni, G., Pennec, X.: Mapping the effects of $A\beta_{1-42}$ levels on the longitudinal changes in healthy aging: hierarchical modeling based on stationary velocity fields. In: MICCAI. pp. 663–670. LNCS, Springer (2011)
13. Lorenzi, M., Ayache, N., Pennec, X.: Regional flux analysis of longitudinal atrophy in Alzheimer's disease. In: MICCAI. LNCS, Springer (2012)
14. Mueller, S., Weiner, M., Thal, L., et al.: The Alzheimer's disease neuroimaging initiative. Neuroimaging Clin. 15, 869–877 (2005)
15. Patenaude, B., Smith, S., Kennedy, D., Jenkinson, M.: A bayesian model of shape and appearance for subcortical brain. NeuroImage In press (2011)
16. Resnik, S., Goldszal, A., C., Davatzikos, Golski, S., Kraut, M., Metter, E., Bryan, R., Zonderman, A.: One year age changes in MRI brain volumes in older adults. Cerebral Cortex 10, 464–472 (2000)
17. Ridha, B., Barnes, J., Bartlett, J., Godbolt, A., Pepple, T., Rossor, M., Fox, N.: Tracking atrophy progression in familial Alzheimer's disease: a serial MRI study. Lancet Neurol 5, 828–834 (2006)
18. Schott, J., Bartlett, J., Barnes, J., Leung, K., et al.: Reduced sample sizes for atrophy outcomes in Alzheimer's disease trials: baseline adjustment. Neurobiol Aging 31(8), 1452–1462 (2010)
19. Smith, S., Zhang, Y., Jenkinson, M., Chen, J., Matthews, P., Federico, A., Stefano, N.D.: Accurate, robust, and automated longitudinal and cross-sectional brain change analysis. NeuroImage 17 (2002)
20. Thompson, P., Ayashi, K., Zubicaray, G., et al.: Dynamics of gray matter loss in Alzheimer's disease. The Journal of Neuroscience 23, 994–1005 (2003)
21. Vercauteren, T., Pennec, X., Perchant, A., Ayache, N.: Symmetric Log-domain diffeomorphic registration: A Demons-based approach. MICCAI 5241, 754–761 (2008)
22. Yushkevich, P., Avants, B., Das, S., J.Pluta, Altinay, M., Craige, C.: Bias in estimation of hippocampal atrophy using deformation-based morphometry arises from asymmetric global normalization: An illustration in ADNI 3 T MRI data. NeuroImage 50(2), 434–445 (2010)